ELSEVIER

www.elsevier.nl/locate/carres

Carbohydrate Research 332 (2001) 285–297

CARBOHYDRATE RESEARCH

Structural analyses of two arabinose containing oligosaccharides derived from olive fruit xyloglucan: XXSG and XLSG

Esther Vierhuis,[a] William S. York,[b] V.S. Kumar Kolli,[b] Jean-Paul Vincken,[a] Henk A. Schols,[a] Gert-Jan W.M. Van Alebeek,[a] Alphons G.J. Voragen[a,*]

[a]*Laboratory of Food Chemistry, Department of Agrotechnology and Food Sciences, Wageningen University, Bomenweg 2, 6700 EV Wageningen, The Netherlands*

[b]*Complex Carbohydrate Research Center and Department of Biochemistry and Molecular Biology, University of Georgia, 220 Riverbend Road, Athens, GA 30602, USA*

Received 21 November 2000; accepted 27 March 2001

Abstract

Xyloglucan oligosaccharides were prepared by *endo*-(1→4)-β-D-glucanase digestion of alkali-extractable xyloglucan from olive fruit and purified by a combination of gel-permeation (Bio-Gel P-2) chromatography and high-performance anion-exchange chromatography. The two most abundant oligosaccharides were converted to the corresponding oligoglycosyl alditols by borohydride reduction and structurally characterised by NMR spectroscopy and post-source decay (PSD) fragment analysis of matrix-assisted laserinduced desorption/ionisation time-of-flight (MALDI-TOF) mass spectra. The results revealed that olive fruit xyloglucan is mainly built from two novel oligosaccharides: XXSG and XLSG. The structure of the oligosaccharides confirmed the presence of a specific xyloglucan in olive fruit with α-L-Ara*f*-(1→2)-α-D-Xyl*p* sidechains as was suggested previously. The presence of such sidechains is a common feature of xyloglucans with an XXGG core produced by solanaceous plants but has not been demonstrated for other dicotyledonous plants, which have in general an XXXG core. Direct treatment of cell wall material from olive fruit with pectin degrading enzymes in combination with *endo*-(1→4)-β-D-glucanase revealed that some of the arabinose residues of the oligosaccharides XXSG and XLSG are substituted with either 1 or 2 *O*-acetyl groups.

Keywords: Olive fruit; Xyloglucan; Oligosaccharides; *O*-Acetyl groups; NMR spectroscopy; MALDI-TOF MS

1. Introduction

Xyloglucans are hemicellulosic polysaccharides found in the primary cell wall of plants and are closely associated with cellulose microfibrils by hydrogen bonds. These noncovalent cross-links between cellulose microfibrils and xyloglucan molecules play a major role in defining the structural properties of plant cell walls and the regulation of growth and development of dicotyledonous plants.[1–3] In addition to this structural role, xyloglucans can be present as a food reserve in seeds and they can be broken down to oligosaccharides that may act as signal molecules.[4–6]

Xyloglucans have a cellulose-like main chain composed of β-(1→4)-linked D-Glc*p*

* Corresponding author. Tel.: +31-317-482888; fax: +31-317-484893.

E-mail address: fons.voragen@chem.fdsci.wag-ur.nl (A.G.J. Voragen).

0008-6215/01/$ - see front matter
PII: S0008-6215(01)00096-9

residues in which up to 75% of the β-D-Glc*p* residues can be substituted at C-6 with α-D-Xyl*p* residues. Some of the α-D-Xyl*p* residues are extended at C-2 with a monosaccharide (β-D-Gal*p* or α-L-Ara*f*) or disaccharide (α-L-Fuc*p*-(1→2)-β-D-Gal*p*). The distribution of the sidechains is species and tissue specific.[5,7–10] Comparison of known xyloglucan structures revealed that most xyloglucans are composed of either XXXG-type or XXGG-type building units.[11] The letters 'G' and 'X' refer to an unbranched Glc residue and a Xyl–Glc segment, respectively.[12]

Sugar linkage analyses and degradation studies with *endo*-(1→4)-β-D-glucanases indicated a xyloglucan in olive fruit with a specific substitution pattern. It probably consists of XXXG-type building units with both Ara and Gal residues linked to it.[13] So far, Ara-containing sidechains have been described as a common feature for xyloglucans isolated from solanaceous plants which consist of XXGG-type building units.[11] In our previous study, we were not able to establish the exact position of the specific Ara-containing sidechain on the backbone of the xyloglucan oligosaccharides. We now describe the purification and rigorous characterisation of the two most abundant oligosaccharides present in the endo-glucanase digest of xyloglucan from olive fruit.

2. Experimental

Materials.—Olive (*Olea europaea* cv koroneiki) cell wall material was obtained from purple olive fruit by EtOH extraction as described previously.[14] The xyloglucan-rich fraction was obtained by anion-exchange chromatography from a 4 M KOH extract of purple olive fruit.[14] *endo*-(1→4)-β-D-Glucanase V (EndoV) was purified from a commercial enzyme preparation from *Trichoderma viride*.[15] Endo-polygalacturonase (PG) originated from *Kluveromyces fragiles* and pectin methyl esterase (PME) from *Aspergillus niger*.[16] Pectin lyase (PL) was purified from a commercial enzyme preparation of *A. niger*.[17] The pectin lyase preparation contained residual endo-glucanase side activities. These side activities have an identical mode of action towards the xyloglucan-rich fraction obtained from the 4 M KOH extract as EndoV isolated from *T. viride*.

Preparation of olive xyloglucan oligosaccharides from a 4 M KOH extract.—The xyloglucan-rich fraction (50 mg) was dissolved in a 50 mM NaOAc buffer of pH 5.0 containing 0.01% (w/v) NaN_3 and incubated with EndoV. The incubation was performed at 40 °C for 48 h with a substrate concentration of 5 mg/mL. The resulting digest was heated for 15 min at 100 °C to inactivate the enzymes. The xyloglucan digest was applied on a Bio-Gel P-2 column (87 × 2.6 cm, 200–400 mesh, Bio-Rad) and eluted with distilled water at a flow rate of 0.5 mL/min at 60 °C. Fractions of 2.6 mL were collected and analysed for neutral sugar content using colorimetric methods.[14] Appropriate fractions were combined and freeze dried. Fractions 7 and 8 were subjected to preparative high-performance anion-exchange chromatography (HPAEC) using a Thermo Quest P4000 quaternaire gradient pump equipped with a CarboPac PA-1 column (250 × 22 mm; Dionex). Elution took place at 20 °C at a flow rate of 25.0 mL/min. The fractions were subjected to the following NaOAc gradient in 100 mM NaOH: 0→5 min, linear gradient of 0→50 mM NaOAc; 5→35 min, linear gradient of 50→70 mM NaOAc; 35→60 min, linear gradient of 70→74 mM NaOAc, 60→80 min, linear gradient of 74→90 mM NaOAc. After each run the column was washed for 5 min with 100 mM NaOH containing 1 M NaOAc and subsequently equilibrated with the starting eluent for 15 min. Solvents were degassed and stored under He using a Dionex eluent degassing module. The column effluent was monitored using a Dionex pulsed electrochemical detector (PED) in the pulsed amperometric detection (PAD) mode. A reference Ag/AgCl electrode was used containing a gold electrode using the following pulse potentials and durations: E_1 0.1 V and 0.4 s, E_2 0.7 V and 0.2 s, E_3 −0.1 V and 0.4 s. The effluent was neutralised by on-line addition of 5 M HOAc and appropriate fractions (*c*, 6.25 mL) were combined. To desalt the HPAEC fractions, the oligosaccharides were adsorbed on a Sep-Pac

C18 reversed phase cartridge (Waters). The cartridge was washed extensively with distilled water and subsequently eluted with MeOH (80% v/v). The purity of the oligosaccharides was checked by analytical HPAEC.[13]

Preparation of xyoglucan oligoglycosyl alditols.—Xyoglucan oligosaccharides were converted to the corresponding oligoglycosyl alditol derivatives by reduction with $NaBH_4$ (10 mg/mL in 1 M NH_4OH), and the products were isolated by reverse-phase chromatography on an octadecyl silica cartridge (Supelclean LC-18, Supelco), as previously described.[9]

Preparation of olive xyloglucan oligosaccharides from cell-wall material.—Cell-wall material of olive fruit (150 mg) was suspended in 6.5 mL of a 50 mM NaOAc buffer of pH 5.0 containing 0.01% (w/v) NaN_3 and treated with a combination of PG, PME and PL to digest the pectic polymers. Oligosaccharides from xyloglucan were released by the residual endoglucanase side activity in the PL preparation The incubation was performed at 40 °C for 24 h. The resulting digest was heated for 15 min at 100 °C to inactivate the enzymes. To remove residual polymeric material from the digest, an EtOH precipitation (60% v/v) was performed. Subsequently, the supernatant was dried, dissolved in 2 mL distilled water and applied on a Sep-Pac C18 reversed phase cartridge (Waters). The cartridge was washed extensively with distilled water to remove salts and eluted with MeOH (20% v/v).

Analytical methods — the neutral sugar composition.—The neutral sugar composition of the fractions was determined by gas chromatography according to Englyst and Cummings[18] using inositol as an internal standard. The samples were treated with 1 M H_2SO_4 for 3 h at 100 °C. The released constituent sugars were analysed as their alditol acetates.

Matrix-assisted laser-induced desorption/ionisation time-of-flight mass spectrometry (MALDI-TOF MS).—MALDI-TOF mass spectrometry in the reflector mode was performed using a Voyager-DE RP Biospectrometry Workstation (PerSeptive Biosystems) equipped with a nitrogen laser operating at 337 nm (3 ns pulse duration), a single stage reflector and delayed extraction. The accelerating voltage used was 12 kV and the delay time setting was 200 ns. Each spectrum was produced by accumulating data from over 100 laser shots.

MALDI-TOF mass spectra used to determine the glycosyl sequence of oligoglycosyl alditols XXSGol and XLSGol were recorded with post-source decay (PSD) using a Kratos SEQ spectrometer equipped with a nitrogen laser operating at 337 nm (3 ns pulse duration), a curved field reflection and delayed extraction. Each spectrum represents the accumulated data from over 100 laser shots, smoothed using the 'average' function. Alternatively, MALDI-TOF mass spectra used to determine the positions of the *O*-acetyl groups on the native XXSG and XLSG were recorded with PSD using the Voyager-DE RP Biospectrometry Workstation mentioned above.

Sample preparation. The matrix solution was prepared by dissolving 9 mg 2,5-dihydroxybenzoic acid (DHB) and 3 mg 1-hydroxy isoquinoline in 700 μL distilled water and 300 μL MeCN. A 1 μL volume of this solution was placed on the sample plate and mixed with 1 μL of the enzyme digest and allowed to dry at rt. Mass spectra were calibrated with an external standard containing cellodextrins (DP 3–9).

Nuclear magnetic resonance spectroscopy (NMR spectroscopy).—The oligoglycosyl alditol samples were dissolved in 99.6% isotopically enriched ^2H_2O (Cambridge Isotope Laboratories) and lyophilised to replace exchangeable protons with deuterons. The residue was dissolved in 99.96% enriched ^2H_2O (600 μL) and transferred to a 5 mm NMR tube. COSY,[19] TOCSY,[20] NOESY,[21] and HSQC[22] spectra were recorded at 298 K with a Varian Inova 600 NMR spectrometer. The TOCSY mixing time was 94 ms. NOESY spectra were recorded with mixing times of 500 ms. COSY and HSQC were recorded using pulsed field gradients for coherence selection.[23] In a typical two-dimensional (^1H–^1H) spectrum, 512 transients of 1024 data points were recorded with a spectral width of 1800 Hz in both dimensions, and the data were processed with zero filling to obtain a

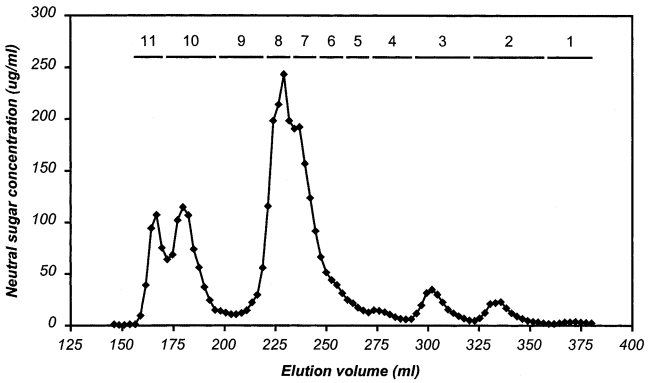

Fig. 1. Elution profile of the EndoV digest of an alkali-extracted xyloglucan-rich fraction from olive fruit on Bio-Gel P-2.

Table 1
Neutral sugar composition (mol%) of Bio-Gel P-2 fractions 7, 8, 10 and 11 and the purified xyloglucan oligosaccharides obtained from an alkali-extracted xyloglucan-rich fraction from olive fruit after treatment with EndoV (tr = trace amount)

Sample	Fuc	Ara	Xyl	Man	Gal	Glc
Bio-Gel P-2 fractions						
Fraction 7	Tr	11	27	8	8	46
Fraction 8	Tr	11	35	3	10	41
Fraction 10	1	11	34	5	10	39
Fraction 11	1	12	40	1	10	36
Purified oligosaccharides						
m/z 1217	0	13	36	0	0	51
m/z 1379	0	11	34	0	10	45

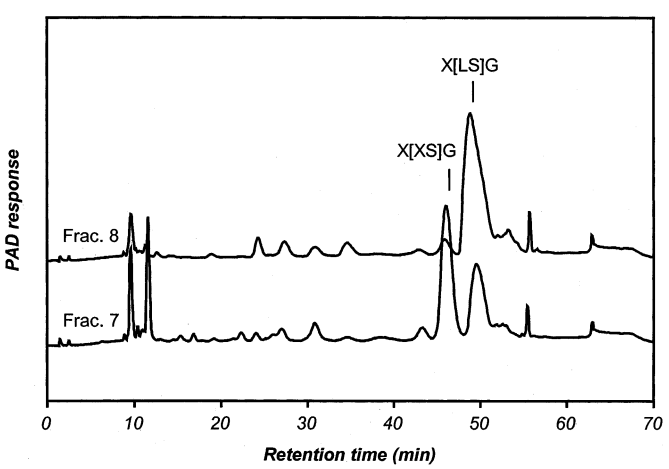

Fig. 2. HPAEC-pattern of Bio-Gel P-2 fractions 7 and 8 obtained from an alkali-extracted xyloglucan-rich fraction from olive fruit after treatment with EndoV.

2048×2048 matrix. Chemical shifts were measured relative to internal acetone at δ 2.225.

3. Results and discussion

Preparation of olive xyloglucan oligosaccharides from a 4 M KOH extract.—The xyloglucan-rich pool obtained by alkali extraction of cell-wall material from olive fruit was digested with *endo*-(1→4)-β-D-glucanase (EndoV). In order to isolate the Ara-containing xyloglucan oligosaccharides of interest (i.e., with three out of four Glc residues bearing a sidechain), the xyloglucan digest was fractionated on Bio-Gel P-2, as shown in Fig. 1. The eluate was pooled into 11 fractions (1: monomers; 11: void volume). The sugar composition of the four main fractions 7, 8, 10 and 11 are given in Table 1. Fractions 7 and 8 contained the oligosaccharides of interest. The MALDI-TOF mass spectrum of fraction 7 showed two main $[M + Na]^+$ ions at m/z 1217 and m/z 1379, corresponding to the glycosyl composition $hexose_4 - pentose_4$ and $hexose_5 - pentose_4$, respectively. The tentative structures X[XS]G and X[LS]G seem most likely for these two ions based on characteristics of the xyloglucan-rich pool, the mode of action of two endo-glucanases towards the substrate, and the molecular masses of the oligosaccharides.[13] The structural elements S and L, containing Ara and Gal, respectively, are indicated in brackets because the exact position of these residues was not known. In principle, the structural elements S and L could also be located at the non-reducing terminus of the xyloglucan oligosaccharides, but the existence of these elements at that position has never been reported before. In addition to the two main $[M + Na]^+$ ions at m/z 1217 and m/z 1379, an ion of intermediate intensity corresponding to an oligosaccharide consisting of six hexosyl residues was present. This oligosaccharide, which lacks pentosyl residues, most probably originated from glucomannan or galactomannan oligosaccharides released by EndoV.[13] The MALDI-TOF mass spectrum of fraction 8 revealed the presence of one main component

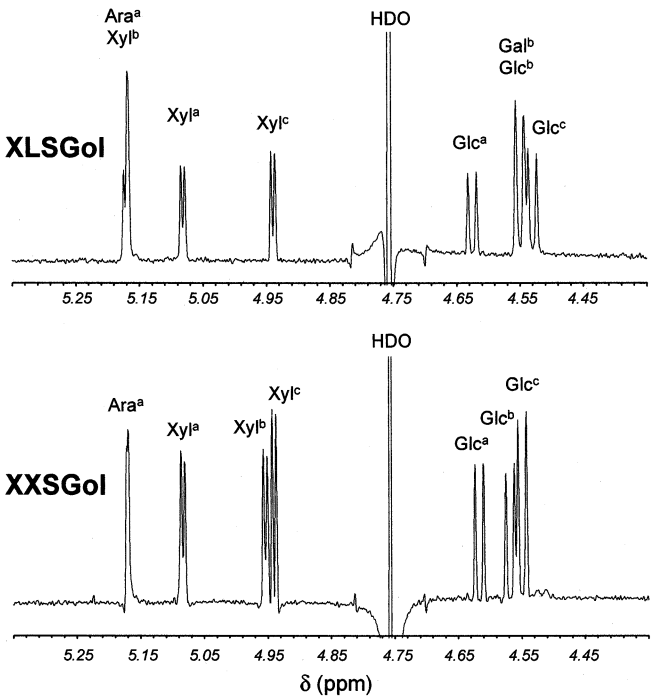

Fig. 3. Anomeric regions of the 1D NMR spectra of the xyloglucan oligoglycosyl alditols XLSGol and XXSGol. The superscript letters (a, b, c) indicate the positions of the glycosyl residues within the oligomer (see footnotes of Table 2).

with m/z 1379. This ion is likely to correspond to X[LS]G.

The elution patterns on HPAEC of Bio-Gel P-2 fractions 7 and 8 are shown in Fig. 2. Besides the major peaks of the oligosaccharides of interest (at 45 and 49 min) the fractions also contained a large number of other oligosaccharides. Further fractionation by preparative HPAEC yielded an oligosaccharide with a Glc:Xyl:Gal:Ara ratio of 4:3:1:1 and an oligosaccharide with a Glc:Xyl:Ara ratio of 4:3:1 (Table 1). The molecular masses of the oligosaccharides, as determined by MALDI-TOF MS, were consistent with these compositions. The oligosaccharides were further characterised using NMR spectroscopy and PSD MALDI-TOF MS in order to determine the exact position of the Ara and Gal residues.

Fraction 10 contained mainly 'dimers' of xyloglucan oligosaccharides, each four Glc residues in its backbone, as determined by HPAEC and MALDI-TOF MS (not shown). Fraction 10 was further digested with EndoV, and MALDI-TOF MS indicated that the major product had a mass (m/z 1379 for the $[M+Na]^+$ ion) that is consistent with the structure X[LS]G. Apparently, EndoV releases X[LS]G from xyloglucan more slowly than X[XS]G, which indicates that the distribution of sidechains substantially affects the rate at which this enzyme attacks specific sites on the xyloglucan backbone.

The xyloglucan-rich pool was not completely degraded by EndoV, as some material eluted in the void volume of the column (Fig. 1; fraction 11). Sugar analysis of fraction 11 (Glc:Xyl:Gal:Ara ratio of 36:40:10:12) indicated the presence of larger oligomeric xyloglucan fragments and a small amount of xylan. Further digestion of this fraction with EndoV also produced a fraction with one main component (m/z 1379), which confirmed the tendency of EndoV to release X[LS]G more slowly than X[XS]G.

NMR spectroscopy of the olive xyloglucan oligoglycosyl alditols.—The presence of two different anomeric forms at the reducing end of the olive xyloglucan oligosaccharides complicated their analysis by NMR spectroscopy, and a complete NMR assignment of these reducing oligosaccharides was not achieved. Therefore, the oligosaccharides were converted to the corresponding oligoglycosyl alditols (OAs) by reduction with $NaBH_4$. The 1D (Fig. 3) and 2D homonuclear NMR spectra (COSY, NOESY, TOCSY) of both OAs, and the $^1H-^{13}C$ HSQC spectrum of the Gal-containing OA were recorded. Analysis of these spectra, in light of a large number of previously reported assignments[8,9,24] for structurally related OAs, allowed all of the ^1H and ^{13}C resonances of the Gal-containing OA and most of the ^1H resonances of the other OA to be assigned (Tables 2 and 3). The general approach was to assign the resonances of the isolated spin systems (each corresponding to a glycosyl residue of the oligomer) by measuring homonuclear scalar coupling constants and tracing scalar connectivity in the COSY and TOCSY spectra. The ^{13}C-resonances of the Gal-containing OA were then assigned by virtue of one-bond heteronuclear ($^1H-^{13}C$) scalar coupling observed in the HSQC spectrum. Glycosidic linkages between residues of the OAs were established by analysis of their NOESY spectra (as described next).

Dipolar $^1H-^1H$ interactions in the OAs were detected as crosspeaks in the NOESY spectra of the OAs. The observation of a crosspeak in the NOESY spectrum indicates that the two interacting protons are in close proximity to each other, which usually occurs because they reside within a single glycosyl residue or within two residues that are glycosidically linked to each other. Although an inter-residue crosspeak in the NOESY spectrum is evidence for a glycosidic linkage, it cannot be taken as proof of the linkage, as NOEs are occasionally observed for pairs of protons that are in close proximity even though they reside within residues that are not glycosidically linked to each other. Nevertheless, all of the NOE crosspeaks listed in Table 3 are consistent with the proposed OA structures XXSGol and XLSGol.

It should be noted that, although the β-Glc*p* residues in the backbone of xyloglucan OAs are connected via (1→4) linkages, a relatively weak NOE is often observed between H-1 of one β-Glc*p* residue and one or both of the protons on C-6 of the β-Glc*p* residue to which it is linked (W.S. York, unpublished results). These NOEs are consistent with the hypothesis that the xyloglucan backbone is (at least transiently) 'twisted' in solution, as has been proposed on the basis of conformational

Table 2
NMR resonance assignments* for the xyloglucan oligoglycosyl alditols XLSGol and XXSGol

	H-1′	H-1	H-2	H-3	H-4	H-5	H-5e	H-6 pro-R	H-6 pro-S
XLSGol									
Glcol	3.687	3.743 (na)[e] 63.3	3.92 (na) 73	3.88 (na) 70.2	3.955 (na) 81.0	3.956 (na) 72.1		3.740 (na) 62.8	3.852
Glc[a]		4.626 (8.0) 103.2	3.421 (9) 73.7	3.675 (sc)[d] 75.9	3.685 (10) 80.4	3.796 (na) 74.6		3.922 (na) 67.5	3.972
Glc[b]		4.548 (8) 103.3	3.404 (9) 73.5	3.664 (sc) 74.9	3.655 (na) 80.6	3.885 (sc) 74.4		3.92 67.5	3.969
Glc[c]		4.531 (8.0) 103.8	3.336 (9) 73.7	3.51 (sc) 76.3	3.52 (na) 70.3	3.694 (5, <3) 75.1		3.937 66.7	3.778
Xyl[a]		5.081 (4.0) 99.5	3.572 (10) 79.6	3.782 (9) 72.9	3.76 (10,5) 70.1	3.57 (11) 62.0	3.730		
Xyl[b]		5.172 (4) 99.5	3.667 (10) 81	3.914 (9) 72.7	3.670 (10,na) 70.1	3.570 (11) 62.0	3.725		
Xyl[c]		4.940 (4.0) 99.1	3.538 (10) 72.3	3.736 (9) 73.8	3.617 (na,5) 70.2	3.544 (11) 62.0	3.712		
Gal[b]		4.550 (8) 105.3	3.615 (10) 71.9	3.66 (<4) 73.4	3.922 (<2) 69.4	3.67 (na) 73.4		3.77 (na) 61.7	3.77
Ara[a]		5.169 (<2) 110.1	4.194 (4) 81.8	3.936 (7) 77.2	4.074 (3,6) 84.5	3.849 (12) 62.0	3.711		
XXSGol									
Glcol	na (na)	na (na)	na (na)	na (na)	3.949 (na)	na (na)		na (na)	na (na)
Glc[a]		4.617 (8.0)	3.412 (9.2)	3.657 (9)	3.678 (10)	3.784 (na)		3.924 (na)	3.978
Glc[b]		4.568 (8.0)	3.388 (9.4)	3.672 (10)	3.733 (na)	3.815 (na)		4.012 (na)	3.895
Glc[c]		4.549 (7.8)	3.338 (9)	3.51 (sc)	3.52 (sc)	3.699 (6, <3)		3.937 (12)	3.781
Xyl[a]		5.083 (3.6)	3.576 (10)	3.783 (9)	3.681 (na)	3.57 (na)	3.728		
Xyl[b]		4.953 (3.6)	3.546 (10)	3.729 (9)	3.629 (na)	3.568 (na)	3.72		
Xyl[c]		4.940 (3.6)	3.543 (10)	3.733 (9)	3.621 (na)	3.55 (na)	3.711		
Ara[a]		5.170 (1.5)	4.190 (4.0)	3.938 (6.3)	4.077 (6.3, 3.2)	3.851 (12)	3.712		

* Data includes: ^1H chemical shifts of protons, ^3J for scalar interaction with next higher numbered proton (in parenthesis), and ^{13}C chemical shifts for the directly attached carbon (XLSGol only). Superscript a, b, c indicate the position of the glycosyl residue with respect to the alditol moiety (i.e., Glc[c]→Glc[b]→Glc[a]→Glcol; Xyl[a] is linked to Glc[a]; Ara[a] is linked to Xyl[a]). (d) Strongly coupled proton pairs are indicated as 'sc'. (e) Chemical shifts and scalar coupling constants that were not assigned are indicated as 'na'.

Table 3
Crosspeaks in the NOESY spectra of the xyloglucan oligoglycosyl alditols XLSGol and XXSGol

From	To				
XLSGol					
5.172	3.969	3.92	3.669		
Xyl^{b} H-1	Glc^{b} H-6S	Glc^{b} H-6R	Xyl^{b} H-2		
5.169	3.574				
Ara^{a} H-1	Xyl^{a} H-2				
5.081	3.974	3.923	3.572		
Xyl^{a} H-1	Glc^{a} H-6S	Glc^{a} H-6R	Xyl^{a} H-2		
4.940	3.935	3.778	3.539		
Xyl^{c} H-1	Glc^{c} H-6R	Glc^{c} H-6S	Xyl^{c} H-2		
4.626	3.954	3.797	3.677		
Glc^{a} H-1	Glcol H-4	Glc^{a} H-5	Glc^{a} H-3		
4.550	3.67	3.884	3.972		
4.548	Gal^{b} H-3	Glc^{b} H-5	Glc^{a} H-6S		
Gal^{b} H-1	Gal^{b} H-5				
Glc^{b} H-1	Glc^{b} H-3				
	Glc^{a} H-4				
	Xyl^{b} H-2				
4.531	3.969	3.693	3.655	3.514	
Glc^{c} H-1	Glc^{b} H-6S	Glc^{c} H-5	Glc^{b} H-4	Glc^{c} H-3	
3.937	3.777				
Glc^{c} H-6R	Glc^{c} H-6S				
3.912	3.569				
Xyl^{b} H-3	Xyl^{b} H-5				
XXSGol					
5.170	3.576				
Ara^{a} H-1	Xyl^{a} H-2				
5.083	3.576	3.922	3.978		
Xyl^{a} H-1	Xyl^{a} H-2	Glc^{a} H-6R	Glc^{a} H-6S		
4.953	3.544	3.893	4.013		
Xyl^{b} H-1	Xyl^{b} H-2	Glc^{b} H-6S	Glc^{b} H-6R		
4.940	3.544	3.782(w)			
Xyl^{c} H-1	Xyl^{c} H-2	Glc^{c} H-6S			
4.617	3.949	3.785	3.655	virtual coupling to Glc^{a} H-4	
Glc^{a} H-1	Glcol H-4	Glc^{a} H-5	Glc^{a} H-3		
4.568	3.814	3.670	3.681	Glc^{b} H-3 and Glc^{a} H-4 overlap	
Glc^{b} H-1	Glc^{b} H-5	Glc^{b} H-3	Glc^{a} H-4		
4.549	4.013	3.893	3.735	3.699	3.51
Glc^{c} H-1	Glc^{b} H-6R	Glc^{b} H-6S	Glc^{b} H-4	Glc^{c} H-5	Glc^{c} H-3

The superscript letters a, b, c indicate the positions of the glycosyl residue within the oligomer (see footnotes of Table 2).

energy calculations.[25] If the backbone were flat (like crystalline cellulose) H-1 would not be close enough to H-6′ to generate the observed NOE (W.S. York, unpublished results). The occurrence of NOEs from H-1 to H-6′ thus provides information about the sequence of β-Glc*p* residues in the OA backbone that would otherwise be difficult to establish because the H-1 to H-4′ NOEs (normally used to establish the (1→4) linkages in the backbone) are often in a crowded region of the ^{1}H NMR spectrum. (See, e.g., the crosspeaks between δ 4.55 and 3.67 in the NOESY spectrum of XLSGol, Table 3.) Therefore, the H-1 to H-6′ NOEs observed in the NOESY spectra of the xyloglucan OAs described herein (Table 3) were interpreted as evidence to support the proposed glycosyl sequences for these oligomers.

The chemical shift assignments given in Table 2 are fully consistent with previously published[8,9,24] data for related OAs. Furthermore, these assignments make it possible to deduce additional correlations between the

chemical shifts of diagnostic ^{1}H-resonances and specific structural features in xyloglucan OAs. Specifically, these new assignments will facilitate the rapid structural assignment of Ara-containing xyloglucan OAs in which three contiguous β-Glc*p* residues in the backbone bear an α-Xyl*p* residue at C-6.

MALDI-TOF MS of the olive xyloglucan oligoglycosyl alditols.—The glycosyl sequences of the two OAs were confirmed by MALDI-TOF mass spectrometry, with detection of fragment ions formed by post-source decay (PSD) (Fig. 4). The PSD technique results in the formation of fragment ions derived from both ends of the oligomer and from multiple fragmentation processes.[26] However, the conditions used to record the MALDI-TOF PSD mass spectra reported here resulted in a fragmentation pattern dominated by sequence-specific ions derived from the alditol end of the oligomers. This fragmentation pattern is analogous to that previously reported[8] for the negative-ion FAB mass spectra of xyloglucan OAs recorded using 1-amino-2,3-dihydroxy propane as the liquid matrix. The main difference between the two techniques is that deprotonated 'Y-type' fragment ions[27] dominate the negative-ion FAB

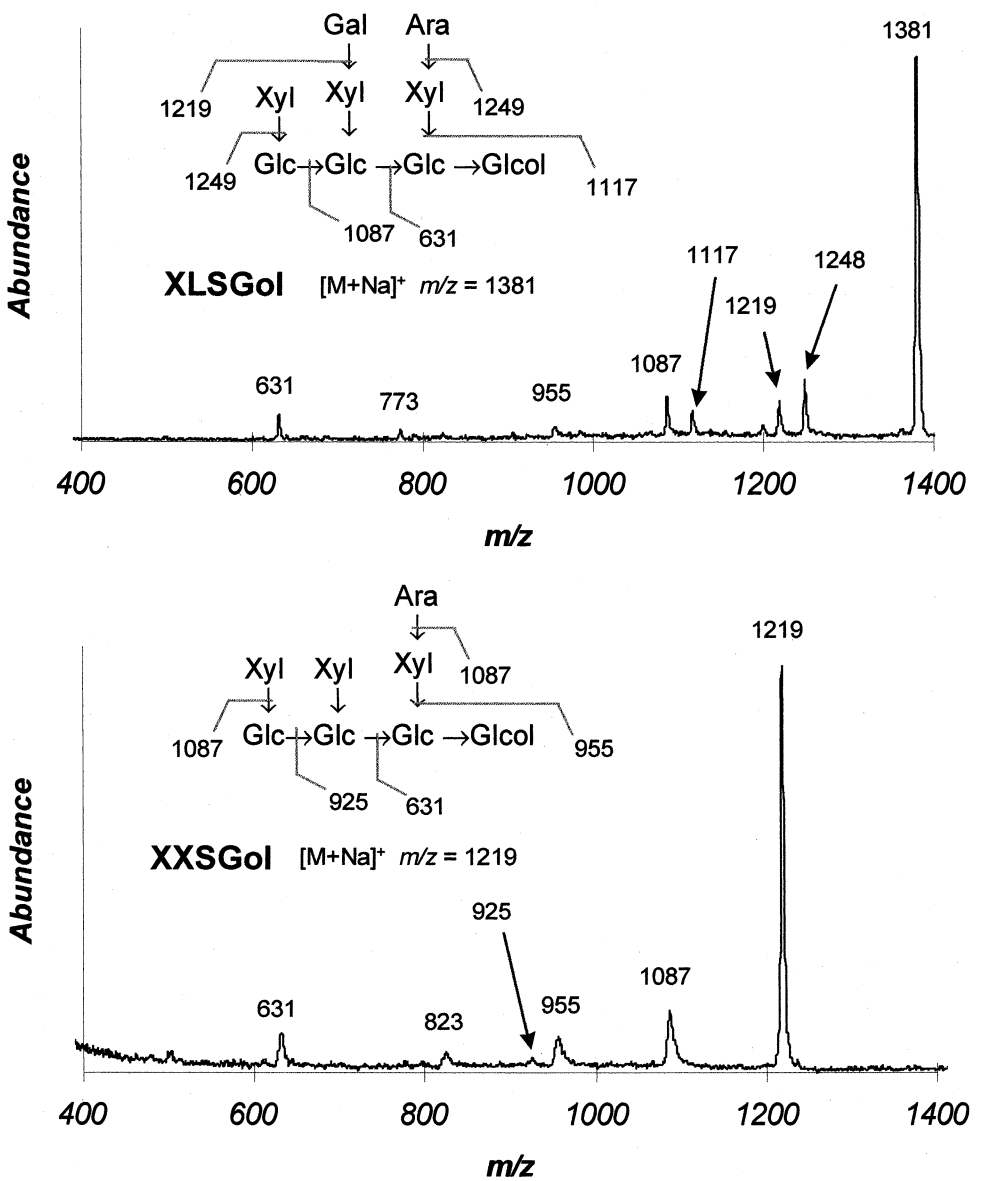

Fig. 4. Post-source decay MALDI-TOF spectra of xyloglucan oligoglycosyl alditols XLSGol and XXSGol. The oligoglycosyl alditols have a mass that is 2 Da greater than the oligosaccharides from which they were derived. The diagnostic ion at m/z 631 indicates that the Ara-containing sidechain is adjacent to the alditol in both of these oligomers.

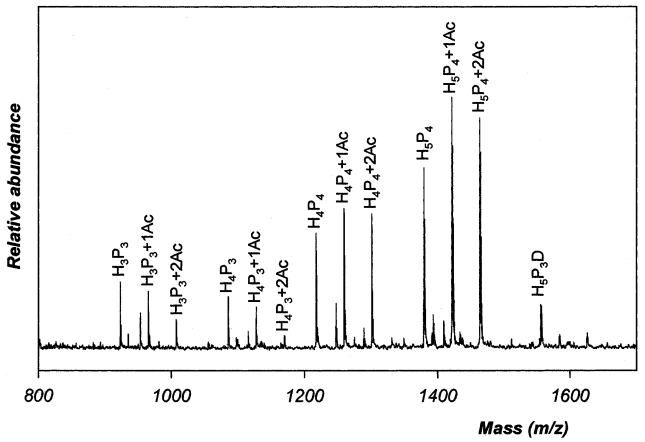

Fig. 5. MALDI-TOF mass spectrum of (O-acetylated) xyloglucan oligomers released from olive fruit cell wall material by digestion with pectin degrading enzymes in combination with endo-glucanase; H = hexose, P = pentose, D = deoxyhexose.

spectra while sodiated 'Y-type' ions dominate the MALDI-TOF PSD spectra. In any case, the dominance of 'Y-type' ions in these spectra facilitate assignment of the glycosyl sequence of the OAs, which would be more difficult if the spectra also contained abundant ions derived from the non-reducing end and/or from multiple fragmentation processes. Although double fragment ions (e.g., at m/z 823 in the spectrum of XXSGol) and ions derived from the non-reducing end (e.g., at m/z 773 in the spectrum of XLSGol) are visible in the MALDI-TOF PSD spectra of the olive OAs (Fig. 4), interpretation of the fragmentation patterns is straightforward and supports the glycosyl sequences proposed on the basis of NMR spectrometry. For example, the diagnostic $[Y + Na]^+$ ion at m/z 631 (pentose$_2$ – hexose – hexitol) in these spectra indicates that the Ara-containing sidechain is adjacent to the alditol moiety in both of the olive OAs.

Structural analyses of olive xyloglucan oligosaccharides substituted with O-*acetyl groups from cell wall material.*—The strong alkaline conditions used to solubilise xyloglucan from cell wall material hydrolyses all ester linkages and consequently O-deacetylates the polymer. To determine if xyloglucan present in olive fruit is O-acetylated, cell wall material was treated directly with enzymes to release xyloglucan oligosaccharides. Pectinases were included to increase the accessibility of the cellulose–xyloglucan network for the glucanases.[28] Analysis of the partially purified xyloglucan oligosaccharides on MALDI-TOF MS showed ions with m/z values corresponding to the two xyloglucan oligosaccharides studied by NMR (m/z 1217 and 1379) and also mono-O-acetylated and di-O-acetylated forms of these xyloglucan oligosaccharides (Fig. 5).

MALDI-TOF PSD analysis of the O-acetylated xyloglucan oligosaccharides XLSG (Fig. 6) and XXSG (not shown) present in the partially purified digest revealed that the *O*-acetyl groups were located on the Ara residue. All fragments containing the Ara residue increased in m/z value with 42 or 84 corresponding to either 1 or 2 *O*-acetyl groups, respectively, whereas fragments without the Ara residue did not change in m/z. The fragment ions without the Ara residue at m/z 773, 1115 and 1247 were very diagnostic, as they showed where the acetate(s) were not located. In particular the ion at m/z 1115, because it clearly indicated that the acetate(s) were present on the sidechain containing two pentosyl residues. The ions at m/z 713 (two acetates), 671 (one acetate) and 629 (no acetates) confirmed the interpretation of the spectra of the oligoglycosyl alditols (Fig. 4; i.e., that the dipentosyl sidechain is attached to the glucosyl residue next to the alditol in XLSGol) and showed that the dipentosyl sidechain was attached to the glycosyl residue next to the reducing glucose in XLSG. The difference of 2 Da between the ion at m/z 629 for the reducing oligosaccharide (XLSG, no acetates) and m/z 631 for the oligoglucosyl alditol (XLSGol) confirmed that these ions were derived from the reducing and alditol end, respectively, of these oligomers. PSD analysis could not reveal the exact position of the *O*-acetyl groups on the Ara residue.

NMR analysis of the partially purified digest indicated that *O*-acetyl substituents were present on the xyloglucan oligosaccharides, but also failed to establish their positions, as the complexity of the spectra was too great. This complexity was probably due to the presence of a large number of differently O-acetylated xyloglucan oligomers.[29]

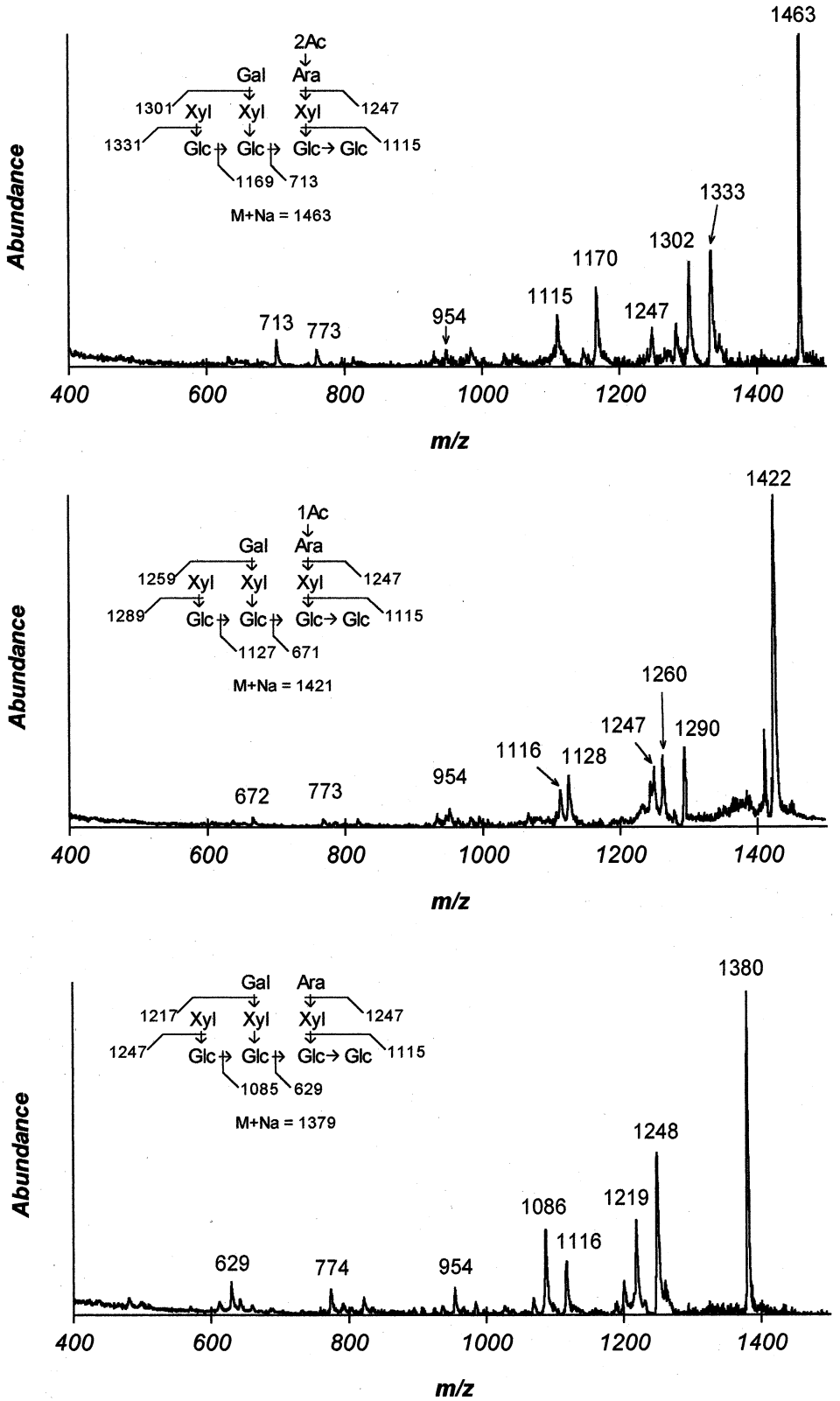

Fig. 6. Post-source decay MALDI-TOF spectra of the xyloglucan oligomer XLSG without *O*-acetyl groups (lower panel), with one (middle panel), and two *O*-acetyl groups (upper panel). DHB (50 mg/mL) was used as a matrix and additional NaCl (50 nmol) was added for optimal cationisation.

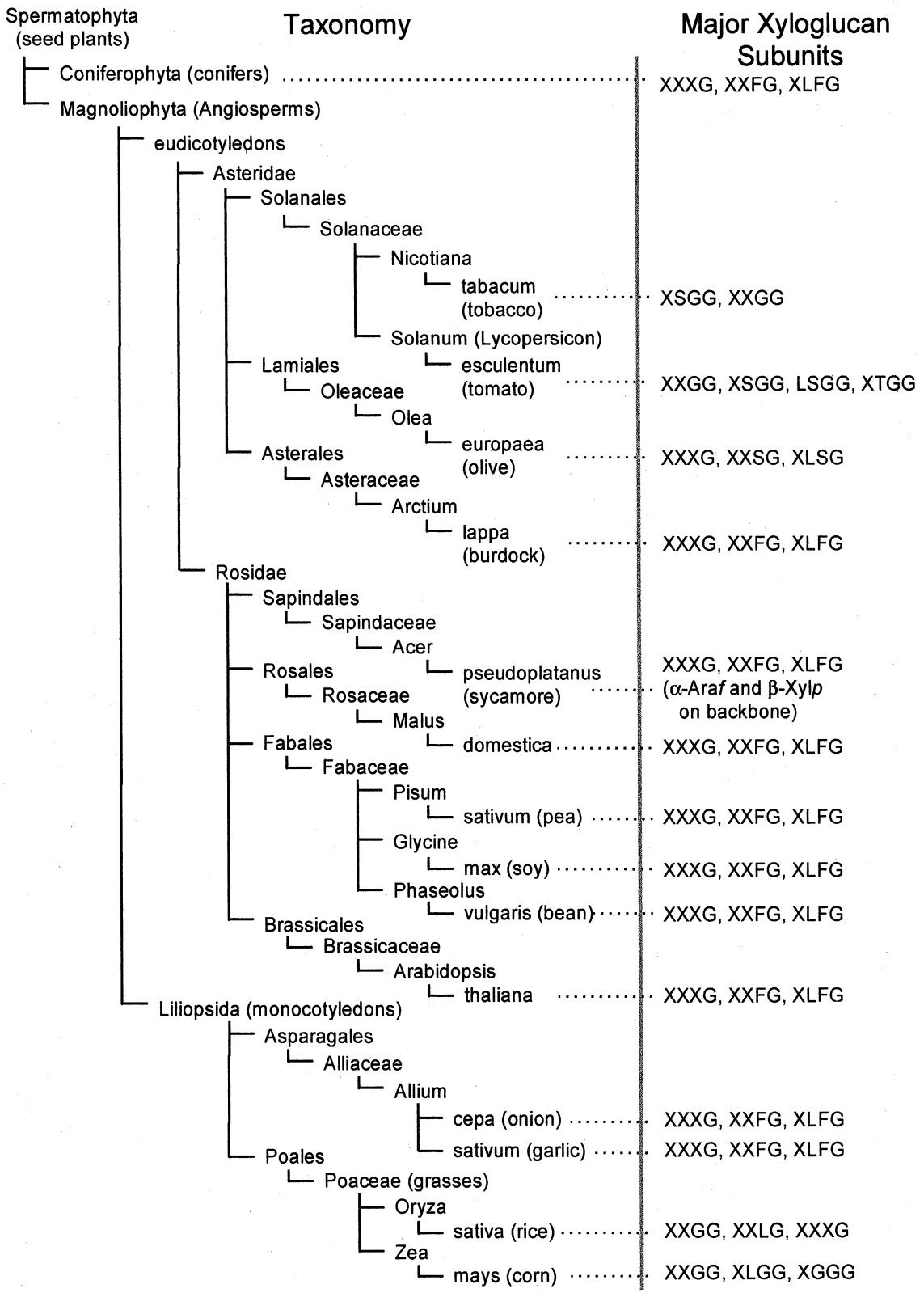

Fig. 7. Phylogenetic relationships of xyloglucan oligosaccharide subunit structures. Each oligosaccharide structure is represented as described in Fry et al.[5] with specific code letters for each segment (G: β-D-Glc*p*-; X: α-D-Xyl*p*-(1→6)-β-D-Glc*p*-; L: β-D-Gal*p*-(1→2)-α-D-Xyl*p*-(1→6)-β-D-Glc*p*-; S: α-L-Ara*f*-(1→2)-α-D-Xyl*p*-(1→6)-β-D-Glc*p*-; F: α-L-Fuc*p*-(1→2)-β-D-Gal*p*-(1→2)-α-D-Xyl*p*-(1→6)-β-D-Glc*p*-; T: β-Ara*f*-(1→3)-α-L-Ara*f*-(1→2)-α-D-Xyl*p*-(1→6)-β-D-Glc*p*-). Phylogenetic relationships are based on the NCBI Taxonomy Browser (http://www.ncbi.nlm.nih.gov/Taxonomy/taxonomyhome.html/).

Correlations between xyloglucan structure and taxonomy.—The primary cell walls of most plants analysed thus far contain fucosylated xyloglucans composed of oligosaccharide subunits (e.g., XXFG) with one unbranched glucosyl residue followed by three branched glucosyl residues[11] (see Fig. 7). This type of branching structure is observed in xyloglucans from a wide range of species, including gymnosperms and both monocotyledonous and dicotyledonous angiosperms. However, the cell walls of some plant species contain xyloglucans with atypical structures. For example, xyloglucans produced by most of the *Poaceae* (grasses) appear to lack Fuc. Another example are dicotyledonous species of the subclass *Asteridae*, some of which produce xyloglucans with α-Ara*f*-(1→2)-α-Xyl*p* sidechains. These include the members of the order Solanales, such as tobacco, potato and tomato, in which the xyloglucan backbone has an unusual branching structure, with two unbranched glucosyl residues followed by two branched glucosyl residues (e.g., XXGG and XSGG).[9] As described here, olive fruit (order Lamiales) contains a xyloglucan whose sidechains contain Ara and lack Fuc, but whose branching structure is more typical, with three out of four glucosyl residues bearing a sidechain. Not all of the *Asteridae* produce unusual xyloglucans, as at least one species (*Arctium lappa*, group euasterids II, order Asterales) produces a typical, fucosylated xyloglucan, in which three of every four glucosyl residues bear sidechains.[30] The structural features of xyloglucan are known to be tissue-specific, so care should be exercised when using these features to determine taxonomic relationships. For example, seed xylogucans often lack fucosyl residues, while leaf tissue from the same plant contains fucosylated xyloglucans.[10] Nevertheless, structural features that are common to the xyloglucans from olive fruit, tomato cells and tobacco cells, for example, are consistent with the inclusion of the orders Lamiales and Solanales in the same taxonomic group, euasterids I. That is, these species all produce xyloglucans with α-Ara*f*-(1→2)-α-Xyl*p* sidechains, which are relatively uncommon. Of these, species in the order Solanales have been shown to produce xyloglucans with an unusual branching pattern that has not been observed in the order Lamiales.

Acknowledgements

This research was supported by the EU (AIR3-CT93-1355) and in part by funds from the National Science Foundation grant MCB-9974673 and by the DOE-funded Center for Plant and Microbial Complex Carbohydrates (DE-FG02-93ER20097). The authors would like to thank the National Institutes of Health, grant no. S10 RR12013 to Dr Ron Orlando (CCRC), for providing the funds to acquire the Kratos SEC mass spectrometer.

References

1. Hayashi, T. *Annu. Rev. Plant Physiol. Plant Mol. Biol.* **1989**, *40*, 139–168.
2. Carpita, N. C.; Gibeaut, D. M. *Plant J.* **1993**, *3*, 1–30.
3. Levy, S.; Maclachlan, G.; Staehelin, L. A. *Plant J.* **1997**, *11*, 373–386.
4. York, W. S.; Darvill, A. G.; Albersheim, P. *Plant Physiol.* **1984**, *75*, 295–297.
5. Fry, S. C. *J. Exp. Bot.* **1989**, *40*, 1–11.
6. McDougall, G. J.; Fry, S. C. *J. Plant Physiol.* **1991**, *137*, 332–336.
7. Kooiman, P. *Recl. Trav. Chim. Pays-Bas* **1961**, *80*, 849–865.
8. York, W. S.; Van Halbeek, H.; Darvill, A. G.; Albersheim, P. *Carbohydr. Res.* **1990**, *200*, 9–31.
9. York, W. S.; Kolli, V. S. K.; Orlando, R.; Albersheim, P.; Darvill, A. G. *Carbohydr. Res.* **1996**, *285*, 99–128.
10. Pauly, M.; Qin, Q.; Greene, H.; Albersheim, P.; Darvill, A.; York, W. S. *Planta* **2001**, *212*, 842–850.
11. Vincken, J.-P.; York, W. S.; Beldman, G.; Voragen, A. G. J. *Plant Physiol.* **1997**, *114*, 9–13.
12. Fry, S. C.; York, W. S.; Albersheim, P.; Darvill, A.; Hayashi, T.; Joseleau, J.-P.; Kato, Y.; Lorences, E. P.; Maclachlan, G. A.; McNeil, M.; Mort, A. J.; Reid, J. S. G.; Seitz, H. U.; Selvendran, R. R.; Voragen, A. G. J.; White, A. R. *Physiol. Plant.* **1993**, *89*, 1–3.
13. Vierhuis, E.; Schols, H. A.; Beldman, G.; Voragen, A. G. J. *Carbohydr. Polym.* **2001**, *44*, 51–62.
14. Vierhuis, E.; Schols, H. A.; Beldman, G.; Voragen, A. G. J. *Carbohydr. Polym.* **2000**, *43*, 11–21.
15. Beldman, G.; Searle-Van Leeuwen, M. F.; Rombouts, F. M.; Voragen, A. G. J. *Eur. J. Biochem.* **1985**, *146*, 301–308.
16. Schols, H. A.; Posthumus, M. A.; Voragen, A. G. J. *Carbohydr. Res.* **1990**, *206*, 117–129.
17. Van Houdenhoven, F. E. A. *Studies on Pectin Lyase, Ph.D. Thesis*; Wageningen Agricultural University: Wageningen, 1975.
18. Englyst, H. N.; Cummings, J. H. *Analyst* **1984**, *109*, 937–942.

19. Bax, A.; Freeman, R. *J. Magn. Reson.* **1981**, *44*, 542–561.
20. Bax, A.; Davis, D. G. *J. Magn. Reson.* **1985**, *65*, 355–360.
21. States, D. J.; Haberkorn, R. A.; Ruben, D. J. *J. Magn. Reson.* **1982**, *48*, 286–292.
22. Bodenhausen, G.; Ruben, D. J. *Chem. Phys. Lett.* **1980**, *69*, 185–189.
23. Keeler, J.; Clowes, R. T.; Davis, A. L.; Laue, E. D. *Methods Enzymol.* **1994**, *239*, 145–207.
24. York, W. S.; Harvey, L. K.; Guillen, R.; Albersheim, P.; Darvill, A. G. *Carbohydr. Res.* **1993**, *248*, 285–301.
25. Levy, S.; York, W. S.; Stuike-Prill, R.; Meyer, B.; Staehelin, L. A. *The Plant J. Cell Mol. Biol.* **1991**, *1*, 195–215.
26. Yamagaki, T.; Mitsuishi, Y.; Nakanishi, H. *Tetrahedron Lett.* **1998**, *39*, 4051–5054.
27. Domon, B.; Costello, C. E. *Glycoconj. J.* **1988**, *5*, 397–409.
28. Vincken, J.-P.; Van den Broek, L. A. M.; Van der Lei, D. D.; Beldman, G.; Voragen, A. G. J. *J. Sci. Food Agric.* **1997**, *73*, 407–416.
29. York, W. S.; Oates, J. E.; Van Halbeek, H.; Darvill, A. G.; Albersheim, P. *Carbohydr. Res.* **1988**, *173*, 113–132.
30. Kato, Y.; Watanabe, T. *Biosc. Biotechnol. Biochem.* **1993**, *57*, 1591–1592.